Catalysis Today 367 (2021) 213–219

Contents lists available at ScienceDirect

Catalysis Today

journal homepage: www.elsevier.com/locate/cattod

Synthesis of butyl glucoside over sulphated Zr-SBA-15 and tungstophosphoric acid incorporated SBA-15 catalysts

Vahide Nuran Mutlu, Selahattin Yılmaz *

İzmir Institute of Technology, Chemical Engineering Department, Gülbahçe Kampüs, Urla İzmir, Turkey

ARTICLE INFO

Keywords:
Glycosidation
Butyl glucoside
Zr-SBA-15
Heteropoly acid incorporated SBA-15
Tungstophosphoric acid

ABSTRACT

Glycosidation of glucose with n-butanol was studied over sulphated Zr incorporated SBA-15 and tungstophosphoric acid (TPA) incorporated SBA-15 catalysts. The catalysts were prepared with different Zr, TPA and SO_4 amounts via hydrothermal synthesis. SBA-15 structure was preserved and Zr and TPA were successfully incorporated. Sulphation improved the acidity of Zr-SBA-15 and the ratio of Brønsted to Lewis acid sites (B/L) increased. Thus, much higher butyl glucoside yields (about 70 %) were obtained over SO_4/Zr-SBA-15 catalysts. However, 15 % activity loss was observed after 2 re-use due to sulphate leaching. TPA-SBA-15 catalysts had the highest B/L and provided very high catalytic activity with butyl glucoside yields above 95 %. The initial rate of butyl glucoside formation over TPA-SBA-15 catalysts were close to that of H_2SO_4. These catalysts were found stable and reusable. Reaction temperature and catalysts amount was studied as the reaction parameters over the most active and selective catalyst.

1. Introduction

Alkyl glucosides are non-ionic chemicals with excellent properties such as low toxicity and good biodegradability. They have attracted the interest of researchers due to their diverse applications as food emulsifiers, personal care products, cleaning agents, textile lubricants, drug carriers and antimicrobial agents [1–3]. Alkyl glucosides are termed as green surfactants since they are synthesized using renewable carbohydrates and alcohols. The first alkyl glucoside was synthesized and identified in the laboratory by Emil Fischer more than 100 years ago [4]. The most common procedure for the alkyl glucoside synthesis was Fischer glycosidation which involves the direct acid–catalyzed acetalization of sugar with an alcohol. The reaction proceeds by nucleophilic attack of the alcohol on the protonated glucose. This nucleophilic attack results in the formation of α and β isomers of alkyl glycosides (Scheme 1). Long chain alkyl glucosides are commonly synthesized by two-step process because of the low solubility of glucose in fatty alcohols. Glucose is acetalized with a short chain alcohol, usually butanol, in the first step. These lower glucosides are more soluble in fatty alcohols and are used in transglycosidation for the synthesis of higher glucosides (Scheme 2) [3,5,6]. The products of glycosidation contains alkyl glycofuranosides and alkyl glycopyranosides as isomer mixtures.

Mineral acids (HCl, HF, and H_2SO_4) and p-toluenesulfonic acid were used as homogeneous catalysts [1–3]. However, they have disadvantages such as waste recovery, environmental hazards, corrosion and difficulties in catalyst recovery and product purification. Enzymes such as β-galactosidase and amilase were also used for the synthesis of alkyl glucosides. Nevertheless, the enzymes are not considered as good candidates for the industry due to their need of mild reaction conditions, unstability and high costs [7,8].

Heterogeneous catalysts were studied as alternatives to homogeneous catalysts and enzymes. Different solid acid catalysts reported in the literature include various zeolites [2,3], Al containing MCM-41 [8], ionic resins [7] and sulfuric acid loaded SiO_2 [5]. Corma et al. (1996) investigated the use of various zeolites such as Na-HY, ZSM-5, H-Mordenite, MCM-22 and HBeta in the synthesis of butyl glucosides. Glycosidation reactions were performed at 110 °C for 4 h and a mixture of butyl glucofuranosides and butyl glucopyranosides were formed [5]. In the continuation of this work, H-Beta catalysts prepared with different Si/Al ratios were tested for the same reactions with the aim of determination of the effect of hydrophobic / hydrophilic character of the catalysts. The results indicated that, the adsorption possess a key role in the reaction because of the presence of the reactants with different polarities. The use of more hydrophobic catalyst declined the adsorption and improved the yield of alkyl glucosides [3].

Heterogeneous catalysts improved the Fischer glycosidation, but

* Corresponding author.
E-mail address: selahattinyilmaz@iyte.edu.tr (S. Yılmaz).

https://doi.org/10.1016/j.cattod.2020.04.060
Received 28 January 2020; Received in revised form 25 April 2020; Accepted 30 April 2020
Available online 6 May 2020

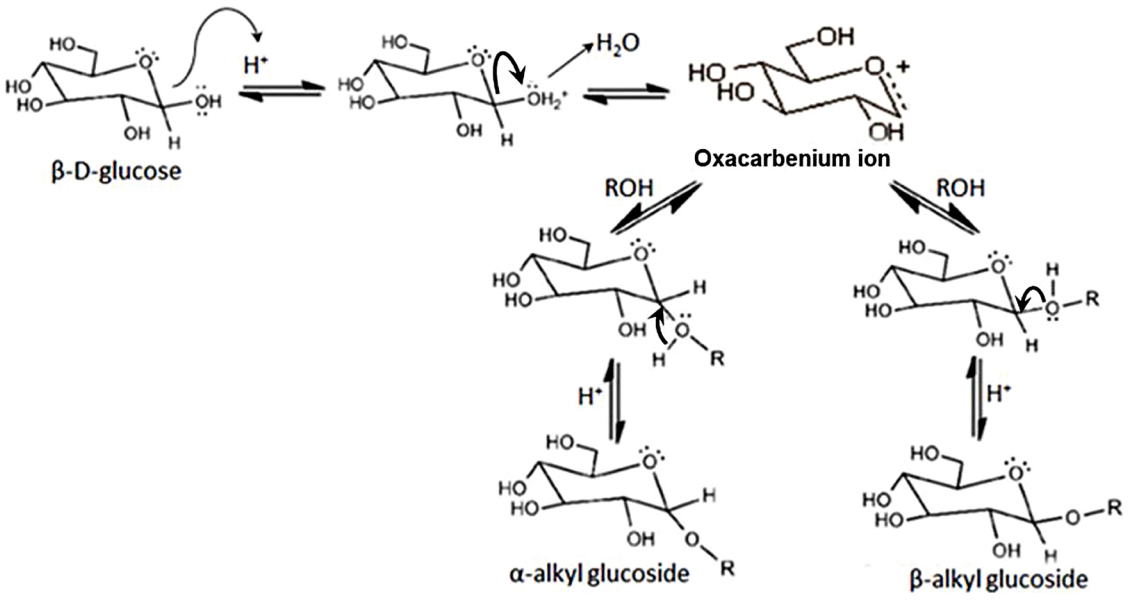

Scheme 1. Fischer glycosidation mechanism.

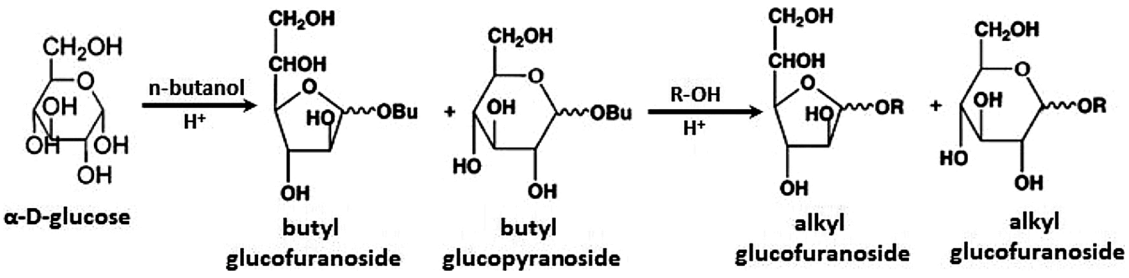

Scheme 2. Two step synthesis of long chain alkyl gluosides.

there is a constant need to develop active, selective and reusable heterogeneous catalysts. The information in the literature suggests that the catalysts used for alkyl glucoside synthesis should have high surface area and pore size, hydrophobic structure and Brønsted acid sites. Mesoporous silicas are catalyst support materials that have been extensively studied in the literature [9–11]. Particularly, SBA-15, which has a hexagonal structure in particular, attracts the researchers with its high surface area and large pore volume, strong hydrothermal stability and modifiable pore size [12]. Different metal ions or active parts have been incorporated into SBA-15 in order to improve the surface acidity and broaden the applications. Zr incorporated SBA-15 catalysts were prepared in the study of Gracia et al. (2009) by hydrothermal synthesis method. Well-structured Zr-SBA-15 mesoporous materials with high surface areas and narrow pore size with both Lewis and Brønsted acid sites were obtained. Sulphation might be applied to enhance the acidity and increasing the amount of Brønsted acid sites. On the other hand, heteropoly tungstophosphoric acid used as a homogeneous catalyst has been found to be an active catalyst for cellulose hydrolysis and glycosidation [13]. Heteropoly acids are known to be strong acid catalysts with high Brønsted acidity resulting from their Keggin ion structure. Even so, the main concern about using heteropoly acids is the reusability since leaching is a common problem with impregnated catalysts [14, 15].

In the present work, sulphated Zr incorporated SBA-15 and tungstophosphoric acid (TPA) incorporated SBA-15 catalysts were reported for the synthesis of butyl glucosides for the first time. Effects of the amount of Zr and TPA, and sulphation on the catalyst properties, activity and butyl glucoside yield were investigated.

2. Experimental

2.1. Catalyst preparation

2.1.1. Preparation of SO_4/Zr-SBA-15 catalysts

Zr incorporated SBA-15 materials were prepared by hydrothermal synthesis method with two different Zr molar amounts (P123:Si:Zr:H_2O 0.017:1:0.08:220 and 0.017:1:0.1:220). They were named as Zr-SBA08 and Zr-SBA1, respectively. As silica and zirconia source TEOS (Aldrich 98 %) and zirconium(IV) oxychloride octahydrate ($ZrOCl_2.8H_2O$, Sigma Aldrich) were used. For synthesis, structure directing agent, P123 ($EO_{20}PO_{70}EO_{20}$) was dissolved in deionized water at 37 °C. Then, required amount of $ZrOCl_2.8H_2O$ and TEOS were added into the P123 solution and stirred at 37 °C for 24 h. Afterwards the gel formed was transferred into a teflon-lined stainless steel autoclave and kept at 100 °C for 24 h. The product obtained was centrifuged and washed with deionized water to remove the weakly adsorbed ions. This was followed by drying at ambient conditions. Finally, it was calcined at 550 °C for 6 h under air flow.

For sulphation, Zr-SBA-15 catalysts were added to 1 M and 0.5 M H_2SO_4 (15 mL/g) and stirred at room temperature for 1 h. The resultant material was then filtered and dried at 80 °C overnight and calcined in air at 550 °C for 3 h. The catalysts sulphated with 0.5 M H_2SO_4 and 1 M H_2SO_4 were named with the prefix of S05 and S1 respectively.

2.1.2. Preparation of TPA-SBA-15 catalysts

Heteropoly tungstophosphoric acid (TPA) was incorporated into SBA-15 via the direct synthesis route with two different amounts, P123:

Si:TPA:HCl:H_2O of 0.07:4.07:0.03:25.2:840 and 0.07:4.07:0.02:25.2:840. These catalysts were named as TPA-SBA-2 and TPA-SBA-3 respectively. For synthesis, P123 polymer weighing of 4 g was dissolved in water and 120 g of 2 M HCl solution. Afterwards 15 mL of aqueous TPA solution was added dropwise into the polymer solution and the mixture was stirred for 24 h before addition of 8 g of TEOS. After TEOS addition the solution was stirred for 30 min. The mixture was placed an autoclave and kept at 80 °C for 24 h under static condition. After that, the autoclave was cooled and the product was separated by centrifuge and washed with deionized water. After drying at 100 °C overnight, it was calcined in air at 420 °C for 6 h.

2.2. Catalyst characterization

The textural properties of the catalysts were evaluated by N_2 adsorption using Micromeritics ASAP 2010 model static volumetric adsorption instrument at 77 K on samples degassed at 200 °C for 12 h. Low angle X-ray diffraction analysis was performed by CuK_α radiation with a step length of 0.02.

Structural analysis of the catalysts were examined by FTIR spectroscopy using KBr pellet technique with a sample amount of 3 wt%. The spectra was retrieved in the wavenumber range of 400–2000 cm^{-1} with a resolution of 4 cm^{-1} by an infrared spectrometer (Schimadzu FTIR 8400S).

Temperature programmed desorption of ammonia (NH_3-TPD) was carried out using Micromeritics AutoChem II Chemisorption Analyzer instrument. The catalyst sample was heated up to 400 °C with a heating rate of 5 °C/min and kept at this temperature for 30 min under He gas flow of 70 mL/min. Then, the temperature was decreased to 90 °C at a rate of 5 °C/min under He flow of 30 mL/min. After that, the sample was subjected to NH3 – He flow at a rate of 30 mL/min for 30 min. This was followed by degassing at 90 °C under He flow of 70 mL/min for 2 h to remove the physically adsorbed NH_3. The sample was then heated to 700 °C with a heating rate of 10 °C/min while recording TCD signal.

Pyridine adsorption FTIR spectroscopy method was used to determine the Brønsted and Lewis acidity characteristics of the catalysts. For a typical analysis, the catalyst sample was degassed at 300 °C under vacuum (2×10^{-2} mmHg) for 2 h. Afterwards, pyridine saturated He gas mixture was passed over it at 120 °C for 30 min. Then, the physiosorbed pyridine was removed by keeping the sample under N_2 flow of 30 mL/min for 2 h at 120 °C. IR spectra were obtained by Shimadzu FTIR 8400S model Fourier Transformed Infrared Spectrometer between 400 and 4000 cm^{-1} using 3 wt% sample pellets prepared with KBr.

Elemental analysis of the catalysts was carried out by ICP-OES. The samples were melted with lithium metaborate and lithium tetraborate at 1000 °C for 1 h and digested in 5 wt% HNO_3 prior to analysis.

Thermogravimetric analysis was performed by Shimadzu TGA-51 instrument by heating from room temperature to 1000 °C at a ramp rate 5 °C/min under N_2. The samples were kept in a desiccator for 1 day before TGA analysis.

2.3. Catalytic tests

Heterogeneous catalysts were tested in 100 mL round bottom flask equipped with a condenser at 117 °C under N_2 atmosphere for 6 h. The stirring rate for the magnetic stirrer was 1000 rpm. The glucose/n-butanol mole ratio was 1/40 and the catalyst weight was 20 % wt of glucose amount.

Product analysis was performed at 50 °C with 3 mM H_2SO_4 as the mobile phase using Thermo Hyperez (30 cm * 0.77 cm) column by Agilent 1100 series HPLC equipment. Two isomers, butyl glucofuranoside (BGF) and butyl glucopyranoside (BGP) were obtained as major products. The equations used to calculate the glucose conversion and butyl glucoside (BG) yield were given below.

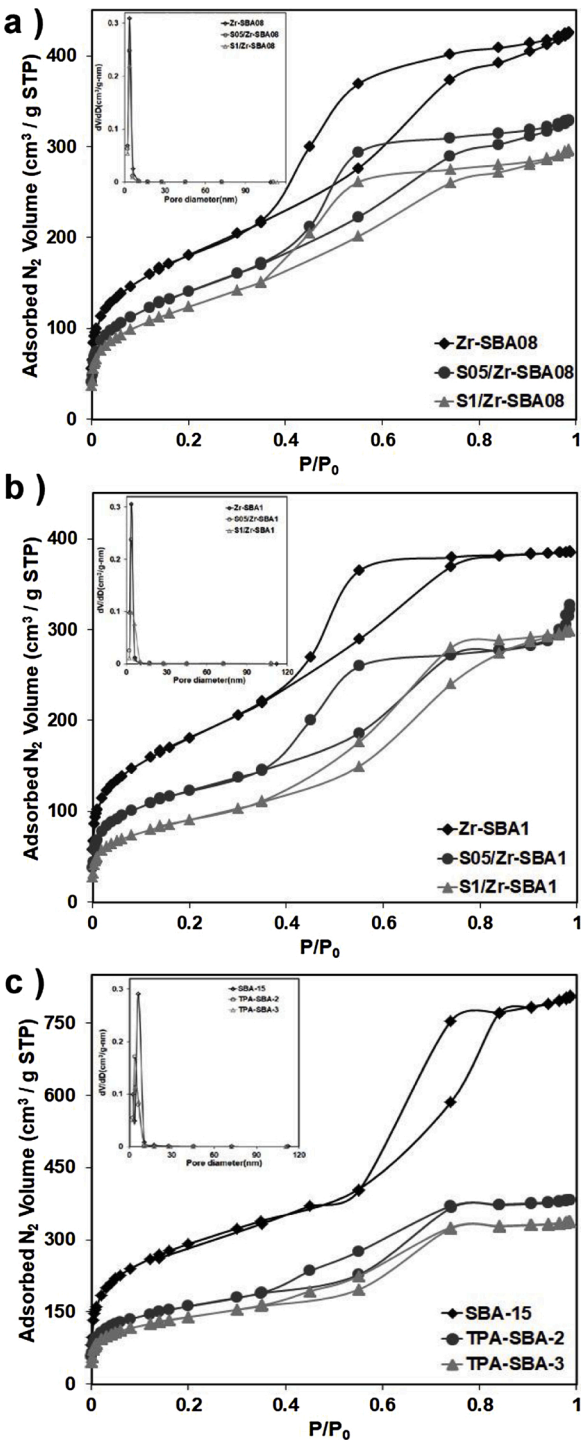

Fig. 1. N_2 adsorption-desorption isotherms and pore size distributions of the catalysts prepared.

$$Glucose\ conversion\ (\%) = \frac{(C_{Glucose_{in}} - C_{Glucose_{out}})}{C_{Glucose_{in}}} x100$$

$$Yield\ of\ BG\ (\%) = \frac{C_{BG}}{C_{Glucose_{in}}} x100$$

Where $C_{Glucose_{in}}$ and $C_{Glucose_{out}}$ are the initial and final glucose concentration respectively, while C_{BG} is the butyl glucoside concentration.

Table 1
Textural properties and acidities of the catalysts prepared.

Catalysts	S_{BET} (m^2/ g)	d_{BJH} (Å)	d_{100} [a] (Å)	T_w [b] (Å)	Zr/Si[c]	S/Zr[c]	P/Si[c]	W/Si[c]	Acidity (mmol NH_3 / g catalyst)	B/L[d]
SBA-15	1009.3	49.5	88.3	57.2	–	–	–	–	–	–
Zr-SBA08	639.1	34.4	88.3	67.5	0.08	–	–	–	1.81	1.12
Zr-SBA1	554.7	37.7	88.3	64.2	0.11	–	–	–	1.97	0.84
S05/Zr-SBA08	502.8	33.2	84.9	64.8	0.10	0.95	–	–	1.92	1.27
S1/Zr-SBA08	444.8	33.1	83.3	63.1	0.09	1.42	–	–	2.10	1.18
S05/Zr-SBA1	428.7	39.0	90.1	65.0	0.12	0.86	–	–	2.20	1.12
S1/Zr-SBA1	322.5	42.6	91.9	63.6	0.11	1.53	–	–	2.42	1.97
TPA-SBA-2	557.9	40.4	81.7	53.9	–	–	0.002	0.02	1.71	2.05
TPA-SBA-3	497.2	42.6	80.2	50.2	–	–	0.003	0.03	1.81	2.07

[a] Interplanar spacing calculated from Bragg equation: $2d\sin\theta = n\lambda$.
[b] Pore wall thickness $T_w = a_0 - d_{BJH}$ where a_0 is the unit cell parameter $a_0 = 2/\sqrt{3}d_{100}$.
[c] Molar ratio calculated from ICP-OES results.
[d] B/L defined as the ratio of the areas under the peaks at 1540 cm^{-1} to 1445 cm^{-1}.

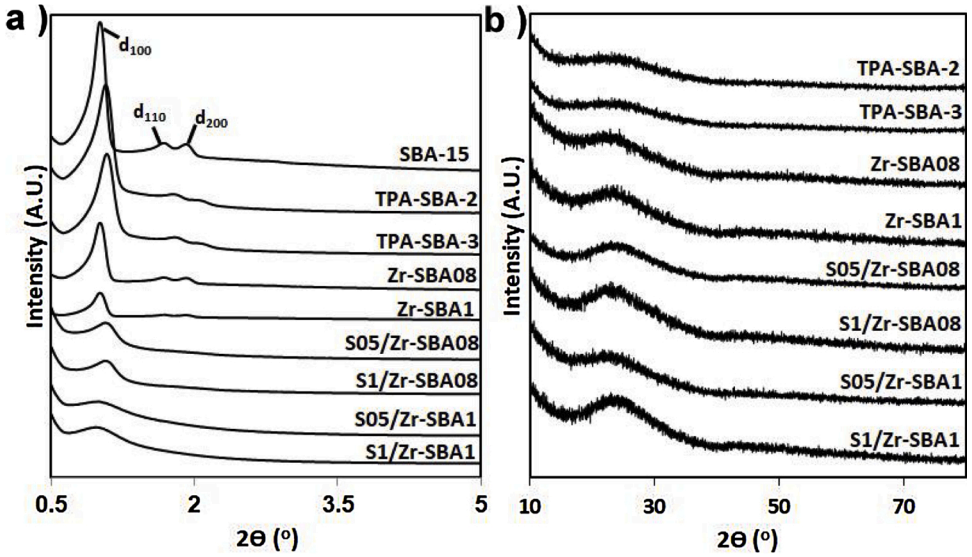

Fig. 2. XRD patterns of the catalysts prepared.

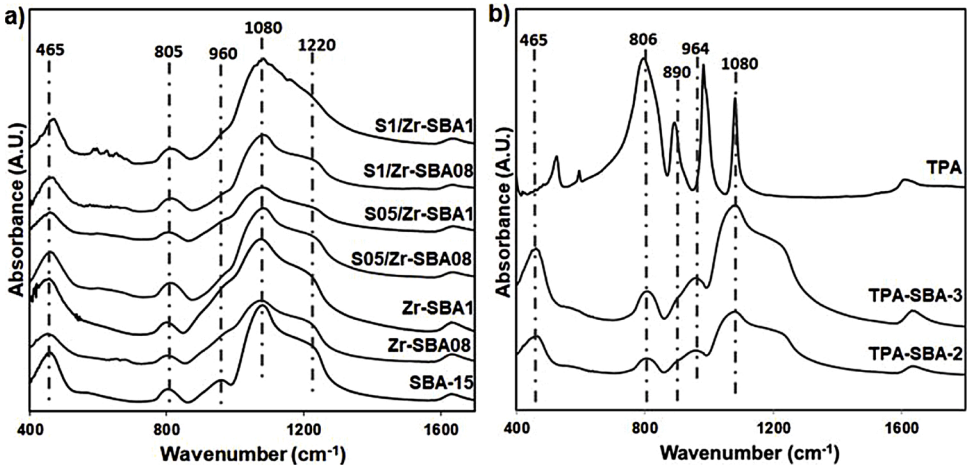

Fig. 3. FT-IR spectra of a)Zr-SBA-15 based catalysts and b) TPA-SBA-15 catalysts.

2.4. Catalyst reusability tests

The used catalysts were filtered out of the reaction mixture and washed with methanol and water. Following that, they were dried at 80 °C for 12 h and tested in the reaction.

3. Results and discussion

3.1. Catalyst characterization

3.1.1. Phase characterization and surface properties

Well-structured Zr-SBA-15 and TPA-SBA-15 mesoporous catalysts

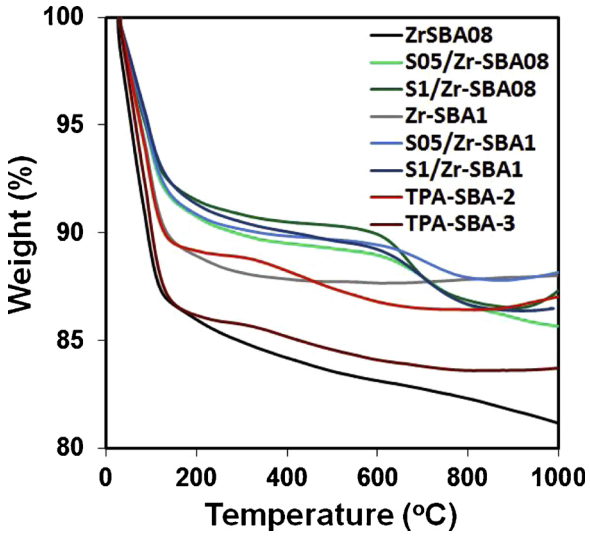

Fig. 4. TGA profiles of the catalysts prepared.

were prepared with narrow pore size distributions and high surface area (Fig. 1 and Table 1). The isotherm and pore size distribution of parent SBA-15 material are also given (in Fig. 1c and Table 1) for comparison purposes. Incorporation of Zr and TPA decreased the surface area of SBA-15. The surface area of the Zr-SBA-15 catalysts decreased further to some extent after sulphation. Zr-SBA-15 based catalysts showed type 4 isotherm with H1 (only for Zr-SBA08) and H2 hysteresis. H1 hysteresis shows the agglomerates or spherical particles arranged in a fairly uniform way, cylindrical pore geometry, indicating relatively high pore size uniformity and facile pore connectivity. On the other hand, H2 hysteresis indicates the presence of network effects. TPA-SBA-15 catalysts showed H3 hysteresis loops, which were attributed to non-rigid aggregates of plate-like particles.

Fig. 2 displays the X-ray diffraction patterns of the catalysts. SBA-15 has one very strong and two weak diffraction peaks within the range of 0.7–2 ° which were attributed to (100), (110) and (200) planes [16]. These are the characteristic peaks indicating the presence of 2D hexagonal lattice structure. TPA-SBA-15 catalysts also showed these three diffraction peaks which proved that the structure of SBA-15 was preserved after the incorporation of TPA. However, the intensity of the (100) diffraction peak significantly decreased after Zr incorporation and subsequent sulphation. However, the peaks indexed to (110) and (200) diffractions were disappeared. This was related to gradual lowering of the long range order. No characteristic peak was observed within the 10–80 ° range. According to the N_2 sorption and low angle XRD results TPA-SBA-15 catalysts had larger pores and thinner pore walls compared to those of Zr-SBA15 based catalysts (Table 1). The results of the elemental analysis showed that the desired amount of Zr and TPA were successfully incorporated.

The structural analysis of SBA-15 and Zr-SBA-15 catalysts determined by FTIR (Fig. 3a). The wide band observed for SBA-15 between 990–1100 cm^{-1} and shoulder around 1200 cm^{-1} indicated the Si—O—Si asymmetric stretching. The peak at 935 cm^{-1} was assigned to Si—OH vibration. These two peaks were broadened and merged by Zr incorporation. Moreover, the band about 960 cm^{-1} is originated from Si—O—Zr vibration and shows that zirconium is successfully incorporated. Sulphation shifted the bands to lower wavelengths which might be due to changes in the length and electronegativity of the bonds [17, 21]. The IR spectra of TPA-SBA-15 catalysts are given in Fig. 3b and compared with the IR spectra of TPA. TPA itself showed IR bands associated with Keggin ion approximately at 800 and 890 cm^{-1} (W—O—W), 980 cm^{-1} (terminal W=O) and 1080 cm^{-1} (P—O in central tetrahedron). All of these bands were observed for TPA-SBA-15 samples with some little shifting in the wavenumbers. This findings demonstrated that the Keggin anion structure of TPA was preserved [18].

Thermal gravimetric analysis (Fig. 4) of the catalysts showed drastic weight loss up to 150 °C. This was attributed to the desorption of adsorbed water molecules. Weight loss due to the adsorbed water was found to be lower for the sulphated Zr-SBA-15 catalysts. This indicated less water was adsorbed over the sulphated Zr-SBA-15 catalysts and so showing more hydrophobic character [19]. A second weight loss region for Zr-SBA-15 based catalysts was observed within the temperature range of 150 °C–450 °C, which was related to the removal of organic molecule residues such as P123 residing in SBA-15 [17]. At temperatures above 600 °C, the sulphated Zr-SBA-15 catalysts showed another weight loss which was considered to be due to decomposition of the sulphates. Thus, it was concluded that the sulphates were stable up to 600 °C. On the other hand TPA-SBA-15 catalysts showed a slight weight loss (1–1.5 %) between 150–250 °C. This corresponds to the loss of water molecules of crystallization of TPA for the formation of Keggin ion structure. Another weight loss region (about 3 %) observed between 300–600 °C. This was attributed to the removal of water contained in TPA molecules inside the mesopores of SBA-15 and organic template. The further weight loss after 600 °C might be due decomposition of TPA [11,20].

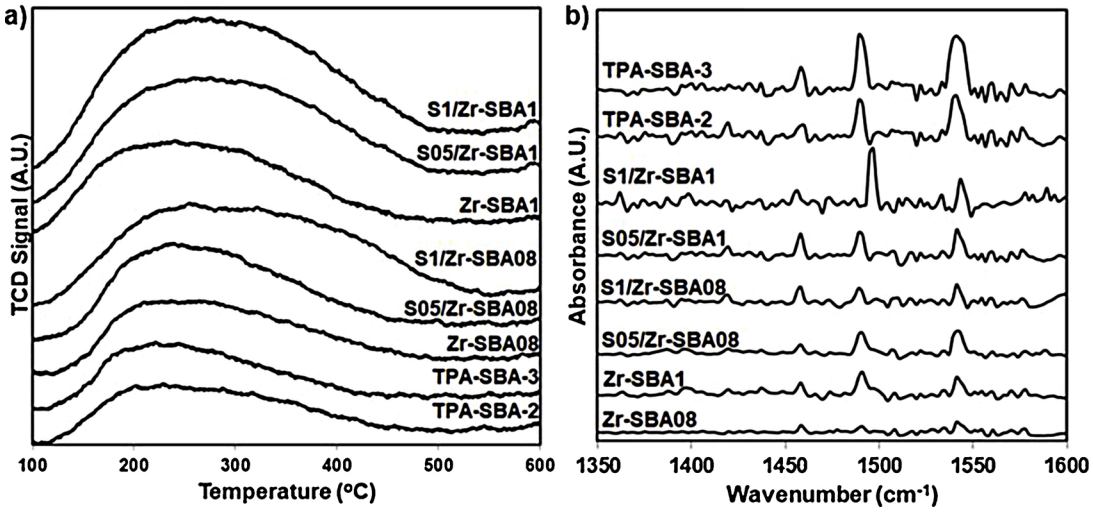

Fig. 5. a) NH_3-TPD profiles and b) pyridine adsorbed FTIR spectra of the catalysts prepared.

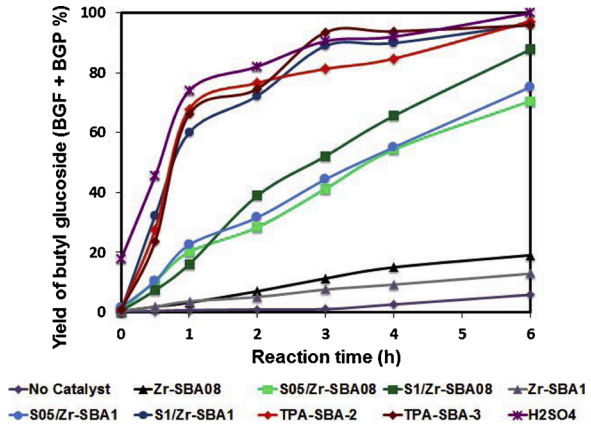

Fig. 6. Butyl glucoside yield obtained over the catalysts.

3.1.2. Acidic properties

The acidity of the catalysts obtained by NH_3-TPD method are given in Fig.5a. A wide peak ranging from 120 to 550 °C was observed for all the catalysts. This showed that all catalysts have weak, medium and strong acid centers. Total acidities of the catalysts were calculated from the area under the peak (Table 1). The acidity of the Zr-SBA-15 catalysts increased with Zr addition and sulphation. TPA-SBA-15 catalysts had lower total acidity compared to that of Zr-SBA-15 based catalysts. The increase in the TPA amount resulted in a slight increase in the total acidity.

The acid site nature of the catalysts were determined as shown in Fig.5b. The peak at 1445 cm^{-1} indicate pyridine coordination on Lewis acid sites, while the peak at 1540 cm^{-1} are attributed to the pyridinium ion bonding to Brønsted acid centers. The peak at 1495 cm^{-1} are related with both Lewis and Brønsted acid sites [20]. The catalysts had Lewis and Brønsted acid sites. The ratio of Brønsted to Lewis acid sites peak areas (B/L) are given in Table 1. The B/L of S1/ZrSBA-1 and TPA-SBA catalysts were much larger than the other catalysts.

3.2. Activities of the catalysts in butyl glucosides formation

Butyl glucosides yield obtained over different catalysts are given in Fig. 6. Preliminary reaction tests were performed without catalyst and with H_2SO_4 for comparison purposes. The yield of BGF was limited to 1.23 % without catalyst, while no BGP can be produced. The use of H_2SO_4 as homogeneous catalyst resulted in the highest glucoside yield (99.9 %) as expected (Table 2).

Zr-SBA08 and Zr-SBA1 catalysts provided very low glucoside yields, maximum of 19.1 % (Table 2). This might be explained by their lower acidity and B/L ratio. Sulphation improved the yield significantly. The BG yield obtained over sulphated Zr-SBA-15 catalysts were above 70 %. When S05/Zr-SBA08 and S05/Zr-SBA1 catalysts were compared, a slight increase in BG yield was observed with the increase in Zr amount.

Table 3
Effect of reaction temperature and catalyst amount on glucose conversion, yield of BGF, BGP and total BG and initial rate of BG formation over TPA-SBA-2 6 h reaction time.

Temperature (°C)	Catalyst amount (% wrt. glucose weight)	Glucose Conversion (%)	BGF Yield (%)	BGP Yield (%)	Total BG Yield (%)
117	20	99.2	27.8	69.4	97.1
100	20	87.5	30.7	53.4	84.1
117	30	99.3	28.2	70.1	98.3

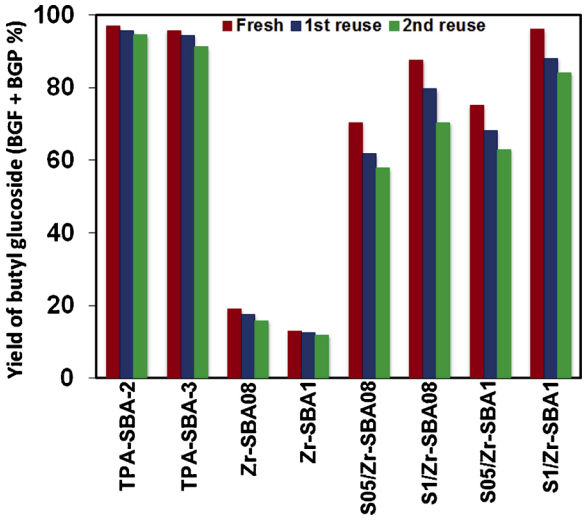

Fig. 7. The reusability tests of the catalysts.

Although the total acidity of S05/Zr-SBA1 was higher than that of S05/Zr-SBA08, the BG yield did not increase significantly due to the lower B/L ratio. The Zr-SBA-15 catalysts with higher sulphate loading provided better catalytic activites as the result of their higher acidities. Among the Zr-SBA-15 based catalysts, the highest yield was obtained over S1/Zr-SBA1 catalyst which was the catalysts with the highest total acidity and more Brønsted acid sites (B/L of 1.97 – Table 1) of this group.

Although TPA-SBA-15 catalysts had lower total acidity, it gave similar BG yields to most acidic Zr-SBA-15 based catalyst (S1/Zr-SBA1). This was result of their B/L ratio. This results confirmed that the Brønsted acid sites were the active sites for glycosidation. The initial rates of BG formation over TPA-SBA-15 catalysts were very close to H_2SO_4. This result showed that TPA-SBA-15 catalyst might be a good alternative to homogeneous acid catalysts.

The effect of reaction temperature and catalyst amount was investigated for the catalyst giving highest yield. The results are given in Table 3. Lower conversion was observed at low temperature and as a

Table 2
Glucose conversion, yield of BGF, BGP and total BG and initial rate of BG formation over catalysts at 117 °C after 6 h reaction time.

Catalysts	Glucose Conversion (%)	BGF Yield (%)	BGP Yield (%)	Total BG Yield (%)	r_0 x10 ^{5} [a] (mol BG min^{-1} g cat^{-1})
No catalyst	7.3	1.2	0	0	0.33
H_2SO_4	100	27.8	72.1	99.9	26.23
Zr-SBA08	32.0	10.2	8.9	19.1	1.35
Zr-SBA1	20.0	6.3	6.6	12.9	1.55
S05/Zr-SBA08	73.2	29.8	40.7	70.5	9.08
S1/Zr-SBA08	90.1	32.1	55.6	87.7	7.27
S05/Zr-SBA1	77.8	30.2	44.9	75.2	9.80
S1/Zr-SBA1	98.9	25.9	70.3	96.2	27.78
TPA-SBA-2	99.2	27.8	69.4	97.1	31.19
TPA-SBA-3	99.1	31.2	64.6	95.8	30.47

[a] r_0 : initial rate of BG formation within 1 h reaction time per g of catalyst.

result lower butyl glucoside yield was obtained. Increasing catalyst amount slightly affected activities and yield obtained. Considering these results, 20 wt% catalyst amount and 117 °C reaction temperature is appropriate for the reaction.

3.3. The reusability of the catalysts

The reusability of the catalysts was determined by testing used catalysts again in the reaction. The yields of BG obtained at the end of re-uses are presented in Fig.7. TPA-SBA-15 catalyst showed only 3 % decrease in BG yield after 2nd re-use which showed stability and reusability of the catalyst. However, the BG yield obtained over sulphated Zr-SBA-15 catalysts decreased about 15 % after the reusability tests. This was determined to be due to the sulphate leaching from the catalyst.

4. Conclusion

Sulphated Zr incorporated SBA-15 (SO_4/Zr-SBA-15) and tungstophosphoric acid incorporated SBA-15 (TPA-SBA-15) catalysts were tested in glycosidation reaction with n-butanol. Zr-SBA-15 catalysts showed very low activity without sulphation. Sulphation improved both acidity and the activity of the Zr-SBA-15 catalysts. TPA-SBA-15 catalysts were found to be very efficient with a catalytic activity close to that of H_2SO_4. The better catalytic activity in glycosidation reaction is related with the higher amount of Brønsted acid sites. Reusability tests proved the stability of TPA-SBA-15 catalysts.

CRediT authorship contribution statement

Vahide Nuran Mutlu: Validation, Investigation, Resources, Visualization, Writing - original draft, Conceptualization, Methodology, Software, Writing - review & editing. **Selahattin Yılmaz:** Conceptualization, Validation, Investigation, Resources, Project administration, Supervision, Visualization.

Declaration of Competing Interest

The authors declare that they have no known competing financial interests or personal relationships that could have appeared to influence the work reported in this paper.

Acknowledgments

This study was supported by The Scientific and Technological Research Council of Turkey (TUBITAK) with project number of 117M160. Their support is gratefully acknowledged. The authors are also thankful to IZTECH environmental Research Center for the product analysis.

References

[1] N. Villandier, A. Corma, ChemSusChem 4 (2011) 508–513.
[2] A. Corma, S. Iborra, S. Miquel, J. Primo, J. Catal. 180 (1998) 218–224.
[3] M.A. Camblor, A. Corma, S. Iborra, S. Miquel, J. Primo, S. Valencia, J. Catal. 172 (1997) 76–84.
[4] E. Fischer, Über die glucoside der alkohole, Ber. Dtsch. Chem. Ges. 26 (1893) 2400–2412.
[5] A. Corma, S. Iborra, S. Miquel, J. Primo, J. Catal. 161 (1996) 713–719.
[6] M.J. Climent, A. Corma, S. Iborra, S. Miquel, J. Primo, F. Rey, J. Catal. 183 (1999) 76–82.
[7] F. Rantwijk, M.W. Oosteromi, R.A. Sheldon, J. Mol. Catal. B: Enzym. 6 (1999) 511–532.
[8] G. Ljunger, P. Adlercreutz, B. Mattiasson, Enzyme Microbial Technol. 16 (1994) 751–755.
[9] J.A. Melero, L.F. Bautista, G. Morales, J. Iglesias, R.S. Vazquez, Chem. Eng. J. 161 (2010) 323–331.
[10] I.K. Mbaraka, D.R. Radu, V.S.Y. Lin, B.H. Shanks, J. Catal. 219 (2003) 329–336.
[11] V. Brahmkhatri, A. Patel, Appl. Catal. A 403 (2011) 161–172.
[12] Y.Q. Zhang, S.J. Wang, L.L. Lou, C. Zhang, S. Liu, Sol. St. Sci. 11 (2009) 1412–1418.
[13] N. Villandier, A. Corma, Chem. Comm. 46 (2010) 4408–4410.
[14] K. Li, J. Hu, W. Li, F. Ma, L. Xu, Y. Guo, J. Mater. Chem. 19 (2009) 8628–8638.
[15] Y. Guo, K. Li, X. Yu, J. Clark, Appl. Catal. A 81 (2008) 182–191.
[16] L. Fuxiang, Y. Feng, L. Yongli, L. Ruifeng, X. Kechang, Microporous Mesoporous Mater. 101 (2007) 250–255.
[17] P. Biswas, P. Narayanasarma, C.M. Kotikalapudi, A.K. Dalai, J. Adjaye, Ind. Eng. Chem. Res. 50 (2011) 7882–7895.
[18] X. Sheng, J. Kong, Y. Zhou, Y. Zhang, Z. Zhang, S. Zhou, Microporous Mesoporous Mater. 187 (2014) 7–13.
[19] S.Y. Chen, L.Y. Jang, S. Cheng, Chem. Mater. 16 (2004) 4174–4180.
[20] P.Y. Hoo, A.Z. Abdullah, Chem. Eng. J. 250 (2014) 274–287.
[21] V.N. Mutlu, S. Yılmaz, Appl. Catal. A 522 (2016) 194–200.